Geospatial Health 2025; volume 20:1362

Optimizing vaccination sites for infectious diseases based on heterogeneous travel modes in multiple scenarios

Wentao Yang,[1,2] Fengjie Wang,[1,2] Yihan You,[2] Zhixiong Fang,[3] Xing Wang,[4] Xiaoming Mei[5]

[1]National-local Joint Engineering Laboratory of Geospatial Information Technology, Hunan University of Science and Technology, Xiangtan; [2]School of Earth Science and Spatial information Engineering, Hunan University of Science and Technology, Xiangtan; [3]Public Health Clinical Center, Xiangtan Central Hospital, Xiangtan; [4]Xintai Land and Space Planning Service Center, Taian; [5]School of Geosciences and Info-physics, Central South University, Changsha, China

Abstract

Equitable spatial accessibility to vaccination sites is essential for enhancing the effectiveness of infectious disease prevention and control. While traffic modes significantly influence the evaluation of spatial accessibility to vaccination sites, most existing studies measure it separately using homogeneous or single travel modes making it challenging to comprehensively understand the overall accessibility and support spatial optimization for vaccination sites. This study proposes to optimize the spatial distribution of vaccination sites based on heterogeneous travel modes in multiple scenarios by a hybrid travel time approach. This was done by first considering heterogeneous travel modes to measure spatial accessibility to vaccination sites followed by spatial optimization using hybrid travel time to determine the optimal configuration of vaccination sites across multiple scenarios. In the study area of Xiangtan, a prefecture-level city in east-central Hunan Province, China, spatial inequality in accessibility to COVID-19 vaccination sites were identified. The public in the Yuhu and Yuetang districts benefit from easy access to vaccination sites, and spatial accessibility within these areas is also equitable. By utilizing spatial optimization under the condition that the addition of a new site would not result in a comprehensive hybrid travel time increase exceeding 0.1%, up to 21 redundant sites were detected among the original ones and when newly added sites were considered, the optimal number of the optimized sites amounted to 124. These findings provide crucial spatial information to support for enhancing the efficiency of infectious disease prevention and control.

Correspondence: Xiaoming Mei, School of Geosciences and Info-physics, Central South University, Changsha, China.
E-mail: 50653551@qq.com

Key words: vaccination sites, spatial accessibility, spatial optimisation, travel mode.

Funding: this study was supported by the National Science Foundation of China (No. 42471509), the Science and Technology Innovation Program of Hunan Province (No. 2023sk2081), the Social Science Achievement Evaluation Committee Project of Hunan Province (No. XSP2023GLC134) and the Scientific Research Fund of Hunan Provincial Education Department (No. 23B0474).

Conflicts of interest: the authors declare no conflict of interest. The funders had no role in the design of the study; in the collection, analyses, or interpretation of data; in the writing of the manuscript, or in the decision to publish the results.

Availability of data and materials: all data generated or analyzed during this study are included in this published article.

Acknowledgements: the authors would like to deeply appreciate the editor (Prof. Robert Bergquist) and the reviewer for their helpful comments.

Received: 7 November 2024.
Accepted: 18 January 2025.

Geospatial Health 2025; 20:1362
doi:10.4081/gh.2025.1362

Introduction

Recent decades have witnessed the frequent emerging, novel infectious diseases that pose new challenges to human health and sustainable social development. Vaccination has been established as a crucial and effective strategy in combating these emerging infectious diseases (Yang *et al*., 2020). Not only is the use of more effective vaccines needed to address virus evolution (Wei *et al*., 2023), but the scientific allocation of vaccine resources is also a key factor (Qi *et al*., 2022).

The allocation of vaccine resources presents a complex issue, primarily focused on selecting target population and identifying vaccination sites. During the initial period of vaccine development, supply constraints amplify the critical nature of target population selection. Socio-demographic attributions, including occupation, age and gender, are usually considered foundational components in this selection process (Medlock & Galvani, 2009; Sah *et al*., 2018). Several studies highlight the necessity to prioritize vaccinations according to risk and age (Lee *et al*., 2010; Wallinga *et al*., 2010; Sah *et al*., 2018). Nevertheless, besides social-demographic attributes, it is crucial to consider spatial information in the allocation of vaccine resources. Based on the transmission dynamics of infectious diseases simulated by an agent-based

model, the significance of spatial distribution in the allocation of vaccine resources has been explored, demonstrating that optimizing vaccine resources in a virtual space derived from simulation should consider the spatio-temporal dimension (Tao *et al*., 2018; Grauer *et al*., 2020). However, discrepancies between simulated data and actual geographical data may result in invalid estimations. In a real-world context, Zhou *et al*. (2021) confirmed the necessity of a spatial priority strategy for selecting the target population; moreover, the combination of space and age has been proven to be the most effective approach. Furthermore, spatial optimization of vaccine resources has been shown to significantly reduce associated morbidity and mortality (Scroggins *et al*., 2023).

The spatial distribution of vaccination sites is a critical element associated with the inequity in spatial accessibility, which has to do with access to these sites (Amritpal *et al.*, 2019). Distance-based indicators and spatial interaction methods are commonly utilized to evaluate spatial accessibility (Soukhov *et al*., 2023; Chen & Jia, 2019; Huang *et al.*, 2023). The former methods apply space, time and/or cost between residential locations and the vaccination site to assess spatial accessibility. A further example is the analysis of the inequity in spatial accessibility to vaccination sites in the metropolitan area of Chicago, United States based on the street-network distance (Guhlincozzi & Lotfata, 2022). The focus on measuring the relationship between supply and demand of vaccine resources within a spatial framework is commonly executed through the gravity-based method and the two-step floating catchment area (2SFCA) method (Luo *et al*., 2009; McGrail, 2012; Liang *et al*., 2023). While the racial/ethnic unfairness in spatial accessibility to vaccination sites was identified using the gravity-based method (Liu *et al*., 2022), the 2FSCA method was used for exploration of the inequity in the spatial distribution of vaccination sites in two counties in the United States (Qi *et al*., 2022).

Both methods for measuring spatial accessibility have specific application scopes and are not entirely interchangeable. When vaccine resources are abundant, supply and demand imbalances do not need to be considered. In such cases, distance-based indicators can effectively fulfill this task; otherwise, spatial interaction methods are more appropriate. However, no matter which model is selected, the distances must first be clearly defined. Although network distance is widely utilized as a distance indicator (Liu & Yu, 2012; Polo *et al*., 2013; Wang *et al*., 2021), it is unable to depict the influence of various travel modes on spatial accessibility. To address this limitation, various travel modes have been incorporated into methods for measuring spatial accessibility, allowing for the detection of the potential inequity (Tao *et al*., 2020; Park & Goldberg, 2021). Since the selection of travel modes typically depends on distance and varies among different age groups, spatial accessibility based solely on individual travel modes cannot fully capture the overall characteristic of travel distance or time. Hence, integrating diverse travel modes into travel time or distance is crucial for accurately measuring spatial accessibility to vaccination sites (Lee & Miller, 2018; Amritpal *et al.*, 2019; Xiao *et al*., 2022).

The ultimate goal of measuring spatial accessibility is to facilitate the spatial optimization of vaccination sites, a process involving the identification of a set of vaccination sites from existing and potential ones to either maximize or minimize a given objective (Xiao & Murray, 2019; Fei *et al.*, 2024). Depending on the specific objectives, various location-allocation issues can be categorized, including the Location Set Covering Problem (LSCP) (Church & Murray, 2009), the Maximal Covering Location Problem (MCLP) (Snyder & Haight, 2016), the *p*-center problem (Daskin, 1995) and the *p*-median problem (Hakimi, 1964). The LSCP is formulated to minimize the total cost of facility selection while ensuring the fulfillment of all demands. In contrast, the MCLP seeks to maximize the total demand with no more than *p* facilities, allowing for some demands to remain uncovered. However, a fixed distance should be established to address the demand coverage and it has been proposed to optimize spatial coverage by selecting a fixed number of vaccination sites with a travel threshold set to delineate the service area (Chen *et al.*, 2022).

Given the critical role of vaccination in combating infectious diseases, vaccination sites may not adhere to a fixed service distance, necessitating coverage of demand even in areas distant from these sites. The *p*-center and *p*-median problems provide solutions to this limitation. The former aims to minimize the maximum distance between demands and their nearest vaccination sites, while the latter focuses on minimizing the total or average distance (Xiao & Murray, 2019). In contrast, the *p*-median problem can incorporate distance or cost information for all demands, making it particularly suitable for planning vaccination sites. Despite its potential to optimize the distribution of vaccination sites, the *p*-median problem's application across various scenarios is seldom explored. For instance, without adding new sites, it is vital to assess whether existing vaccination sites are redundant. Furthermore, if new sites are required, identifying optimal locations for these sites becomes essential. In light of the aforementioned challenges, this study investigated the spatial optimization of vaccination sites for infectious diseases based on heterogeneous travel modes in multiple scenarios. Our contributions were threefold: i) introduction of hybrid travel time with the integration of heterogenous travel modes to measure spatial accessibility to vaccination sites; ii) optimization of the spatial distribution of vaccination sites based on the hybrid the travel time and the *p*-median problem in multiple scenarios; iii) proposal of a specific optimization scheme for COVID-19 vaccination sites in the study area.

Materials and Methods

Study area

Xiangtan City, which is located in the east-central part of Hunan Province, China spans latitudes from 27°20′N to 28°05′N and longitudes from 111°58′W to 113°05′W. As a prefecture-level city, Xiangtan administers three county-level cities/counties (Xiangtan, Shaoshan and Xiangxiang) and two districts (Yuhu and Yuetang), covering a total area of 5,005.8 km^2. According to the Seventh National Census of China, the city's permanent population is approximately 2.73 million, with an urban population of 1.77 million. The spatial information of the study area is shown in Figure 1.

Datasets and preprocessing

Five primary dataset categories were used: i) Vaccination site records from 2021 (n=92), including names and spatial coordinates, sourced from the Xiangtan Public Health Center; ii) Road network data obtained from OpenStreetMap (https://www.openstreetmap.org); iii) Demographic yearbook data in 2020 from Hunan Provincial Bureau of Statistics (https://tjj.hunan.gov.cn/), which includes three age groups: children under 16 years, those aged 16 to 60 years, and those older over 60 years; iv) Population distribution data in 2021 at 1-km resolution were downloaded from

Worldpop (https://www.worldpop.org), with the number of different age groups estimated according to the proportion of each age group in the demographic yearbook; v) Questionnaire survey data regarding the acceptable walking time to a vaccination site and the walking speed across three age groups. The main content of the questionnaire is what the longest time that you are willing to walk to a vaccination site is, and approximately 100 samples were obtained for each age group. For all groups, the driving speed on the road network was consistently set at 40 km/h in the study area.

Methodology

The framework for optimizing vaccination sites comprised two key components: the assessment of spatial accessibility and the optimization of spatial distribution, as depicted in Figure 2. The population was segmented into distinct groups according to travel preferences or other pertinent criteria, while the travel modes were categorized into various types (two types of travel modes, namely walking and driving, were considered in this research). The hybrid travel time was calculated by integrating the selection probability of each travel mode for each group with the travel time from demand point i and vaccination site j. The comprehensive travel time used to evaluate spatial accessibility was derived from the hybrid travel time and the population distribution. The method for calculating travel time is introduced under Hybrid travel time based on heterogeneous travel modes below. The p-median problem was employed to optimize the spatial distribution of vaccination sites in multiple scenarios. This study defined two distinct scenarios to achieve different objectives in spatial optimization; the first aimed at identifying optimized and redundant vaccination sites among the original sites, and the second at determining optimized sites from a combined set of original and newly added sites as well as detecting abandoned sites among the original sites. The detailed method for spatial optimization in multiple scenarios is provided under p-median problem in multiple scenarios below.

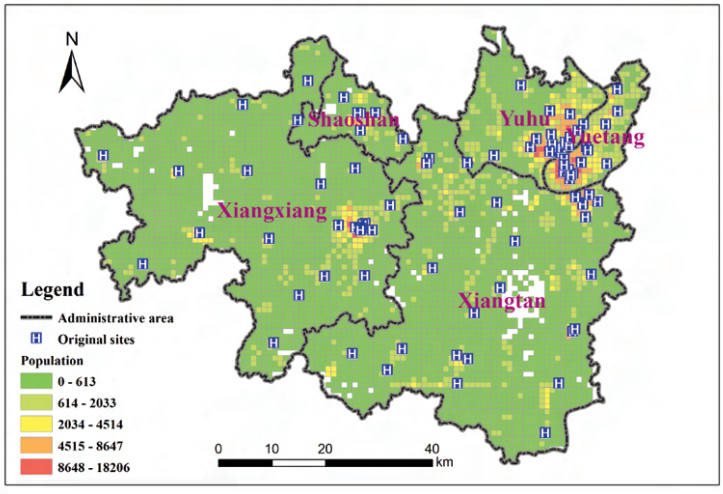

Figure 1. Map of the study area.

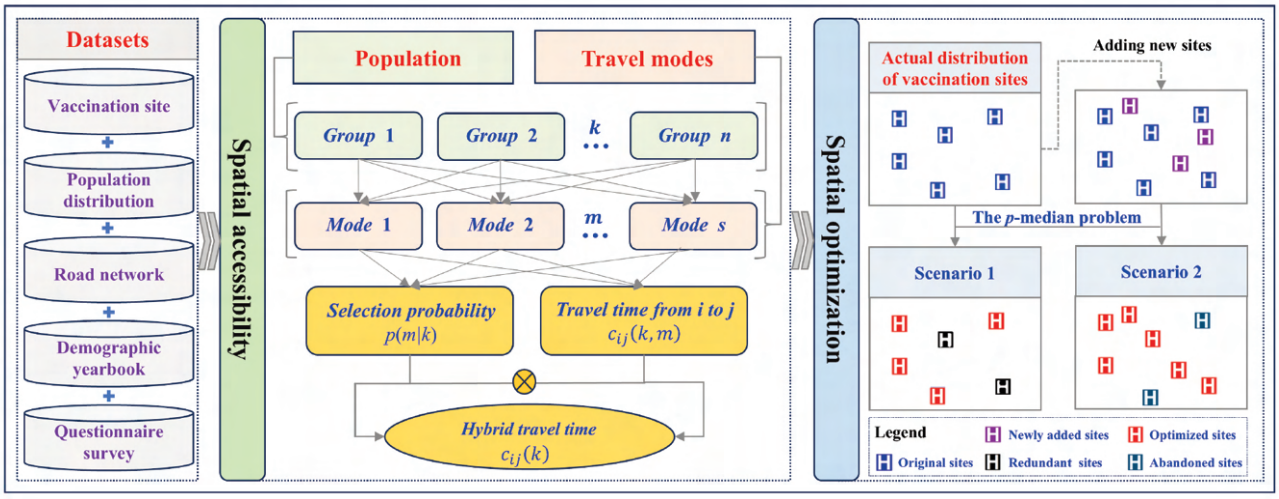

Figure 2. Framework for optimizing vaccination sites in the study.

Hybrid travel time based on heterogeneous travel modes

Travel time is a prevalent metric for quantifying transportation costs, significantly influenced by the chosen travel mode (Yu *et al*., 2018; Huang *et al*., 2022). The research assumed that travel distance and different age groups exhibit varying tolerances for walking distances determine the choice of travel modes (only driving and walking were considered). Due to these differences in the acceptable walking time or distance, the choice of travel modes varied among age groups as done earlier (Yang *et al*., 2024), which means that the selection of travel modes for different age groups should be considered when calculating travel time. Assuming the population is divided into n groups, the travel time $c_{ij}(k, m)$ for a single travel mode m and the k^{th} age group can be expressed as follows:

$$c_{ij}(k,m) = \frac{L_{ij}}{v(k,m)} \quad \text{(Eq. 1)}$$

where L_{ij} represents the network distance between demand point i and vaccination site j; and v (k, m) denotes the average velocity for the travel mode m and the k^{th} age group. It is worth noting that, due to the difficulty in obtaining the proportional information on differ-

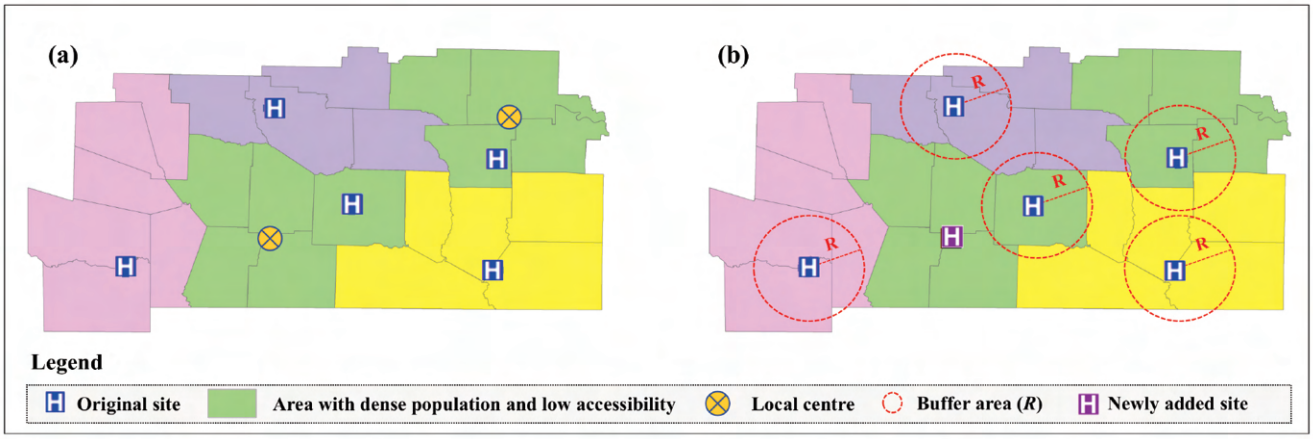

Figure 3. Illustration of temporary vaccination site extraction.

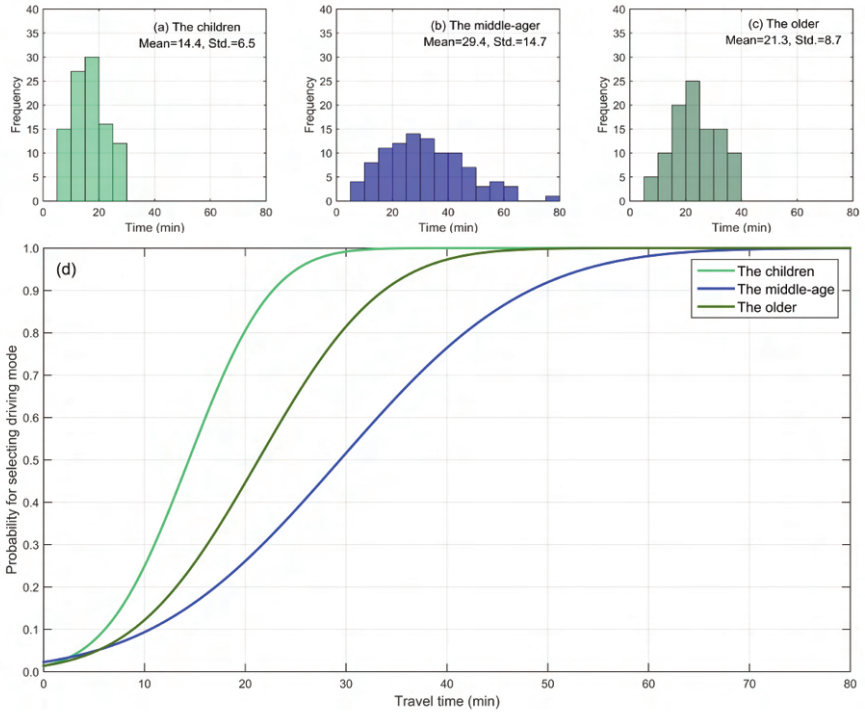

Figure 4. Statistical result giving the probability for selecting the driving mode with different walking time thresholds.

ent driving modes, including private vehicle taxi, and public transportation, this study only used the average road speed to estimate driving time without further discussing specific driving modes. Furthermore, given the spatial differentiation of lifestyle and road network characteristics, the average walking and driving speeds may vary across regions. This study estimated the average velocity of travel modes using a questionnaire survey and road network data. Considering that either driving or walking can be selected for each age group, hybrid travel time for the k^{th} age group can be defined based on the probabilities associated with the choice of travel modes, which is described as follows:

$$c_{ij}(k) = \sum_{m\in\{driving,walking\}} p_k(m)c_{ij}(k,m), \quad \text{(Eq. 2)}$$

where $c_{i,j}(k, m)$ is the travel time or cost between demand point i and vaccination site j for the k^{th} age group based on the travel mode m; and $p_k(m)$ denotes the probability of selecting travel mode m for the k^{th} age group, which satisfies the following condition:

$$\sum_{m\in\{driving,walking\}} p_k(m) = 1. \quad \text{(Eq. 3)}$$

The problem of determining the probability of travel mode choice is complex. Generally, the choice depends on the distance (d_{ij}) between the starting location and the destination. That is, the longer the distance, the more likely it is to choose driving, while the shorter it is, the greater the chance of choosing walking. Thus, if there exists a distance threshold d' to identify walking and driving modes for the k^{th} age group, it can be assumed that walking is preferred if d_{ij} is less than d', otherwise driving would be chosen. If d_{ij} equals d', the probabilities of choosing walking and driving modes are equal, *i.e.* both at 0.5.

We assumed that the distance threshold value only varies across different age groups (*e.g.*, children, middle-aged people and the elderly), with each age group following a Gaussian distribution. If these distance thresholds were inconsistent among different age groups, the cumulative distribution function of a Gaussian distribution that can describe the above characteristics of driving mode choice can be used to calculate the probability, which is defined as:

$$p_k(m = driving|d_{ij}) = \int_{-\infty}^{d_{ij}} \frac{1}{\sqrt{2\pi}\sigma(k)} e^{-\frac{1}{2}\left(\frac{z-\mu(k)}{\sigma(k)}\right)^2} dz, \quad \text{(Eq. 4)}$$

$$p_k(m = walking|d_{ij}) = 1 - \int_{-\infty}^{d_{ij}} \frac{1}{\sqrt{2\pi}\sigma(k)} e^{-\frac{1}{2}\left(\frac{z-\mu(k)}{\sigma(k)}\right)^2} dz, \quad \text{(Eq. 5)}$$

Where $m(k)$ and $s(k)$ are the mean and standard variation of the distance threshold for the k^{th} age group, respectively, which can be estimated from the questionnaire survey or trajectory data. Further, if the population size of each age group in demand point i were known, the comprehensive hybrid travel time c_{ij} between demand point i and vaccination site j can be defined as follows:

$$c_{ij} = \frac{\sum_{k=1}^{n} pop(k,i)c_{ij}(k)}{\sum_{k=1}^{n} pop(k,i)}, \quad \text{(Eq. 6)}$$

Where $pop(k, i)$ represents the number of individuals in kth age group at demand point i. The comprehensive travel time can be regarded as weighted hybrid travel time based on the proportion of each age group.

The p-median problem in multiple scenarios

The p-median problem was used to minimize the overall cost between all demand points and their nearest facilities. Let h represent the size of the vaccination site set $\{s_1, \ldots sh\}$, and define the mathematical expression for the p-median problem ($p < h$) as follows:

$$\min\ TC(p) = \sum_{i=1}^{g}\sum_{j=1}^{h} pop(i)c_{ij}x_{ij}, \quad \text{(Eq. 7)}$$

Subject to

$$x_{ij} \in \{0,1\}, \forall i,j \quad \text{(Eq. 8)}$$

$$y_j \in \{0,1\}, \forall j \quad \text{(Eq. 9)}$$

$$\sum_{j=1}^{h} x_{ij} = 1, \quad \text{(Eq. 10)}$$

$$\sum_{j=1}^{h} y_j = p, \quad \text{(Eq. 11)}$$

$$x_{ij} \le y_j, \forall i,j \quad \text{(Eq. 12)}$$

where the objective (Eq. 7) is to select p sites from the total of h vaccination sites to minimize the total cost $TC(p)$ that describes the total travel time; g the number of demand points; $pop(i)$ the total number of individuals at demand point i; and c_{ij} the comprehensive travel time between demand point i and vaccination site j, as described in (Eq. 6); while x_{ij} represents whether demand point I is served by vaccination site j, whose value can be selected based on the constraint given by (Eq. 8). If x_{ij} is equal to 0, demand point i is served by vaccination site j, otherwise not. Similarly, y_j represents whether vaccination site j is selected, governed by the constraint given by (Eq. 9). If y_j is equal to 1, then vaccination site j is selected, otherwise, not. The constraint given by (Eq. 10) necessitates the allocation of each demand point to a vaccination site, while the constraint given by (Eq. 11) requires that exactly p vaccination sites must be chosen from the vaccination site set. The constraint given by (Eq. 12) ensures that a vaccination site cannot be allocated to an unselected vaccination site. Solving the above optimization model yields the set of optimal vaccination sites, denoted as $OptS(p) = \{s_j | y_j = 1\}$. The Gurobi optimization software (https://www.gurobi.com/) was used to solve the p-median problem in this study. Before describing different scenarios, several definitions should be first given as follows:

Definition 1: (Redundant vaccination sites). These are some original vaccination sites, the removal of which would have no sig-

nificant impact on the total cost.

Definition 2: (Temporary vaccination sites). These are a series of candidate vaccination sites outside the existing sites, with the goal of selecting newly added vaccination sites among them.

Definition 3: (Newly added vaccination sites). These are selected from temporary vaccination sites based on certain principles, which will be combined with original vaccination sites to undergo spatial optimization.

Definition 4: (Optimized vaccination sites). These are the vaccination sites that were ultimately selected through spatial optimization.

Definition 5: (Abandoned vaccination sites). These are some original vaccination sites that were not finally selected through spatial optimization. Unlike redundant sites, abandoned sites can be replaced by some newly added sites to reduce the cost.

Furthermore, various scenarios that describe distinct optimization tasks in practical situations and two commonly-used tasks corresponding to two types of scenarios are delineated as follows:

Scenario 1: This scenario aims to identify redundant vaccination sites within the set of original vaccination sites (denoted as *OriS*). By selecting different values of p, we independently optimized the overall cost by solving the p-median problem and subsequently compare these optimal total cost values to determine redundant sites. According to Definition 1, if redundancy exists among original vaccination sites, it will not significantly affect the total cost. To express this requirement, the condition can be formulated as follows:

$$\frac{TC(p)-TC(p+1)}{TC(p)} \leq \varepsilon, \quad \text{(Eq. 13)}$$

where represents the increment threshold, which was set at 0.1% in this study. Typically, there are numerous values of p that satisfy this condition. Among these values, the minimum value p' is regarded as the optimal number and the corresponding set is referred to as the reasonable or optimized sites (denoted as *OptS*(p')). The set of redundant vaccination sites can be determined by the difference between the set *OriS* and *OptS*(p'), defined as follows:

$$RedS(p') = OriS - OptS(p'). \quad \text{(Eq. 14)}$$

Scenario 2: This scenario aims to identify optimized vaccination sites by newly adding a series of temporary vaccination sites and abandoning some vaccination sites among original sites (denoted as *AbaS*). In this scenario, optimized vaccination sites are obtained from both original and newly added vaccination sites through solving the p-median problem. By comparing the differences between optimized and original sites, abandoned sites can be obtained. Specifically, through the consideration of population distribution and spatial accessibility of original vaccination sites, a series of temporary vaccination sites were extracted and added to the original vaccination sites. We defined temporary vaccination sites as centres within areas characterized by low accessibility and high population density (Low-High areas). It is worth noting that besides Low-High areas, Low-Low, High-Low and High-High areas can also be distinguished but obviously, more attention should be paid to the Low-High areas, as exemplified by the blue areas in Figure 3, which exhibited low accessibility and high population density. Then, the centres in these blue areas can be considered as the added sites in Figure 3(a). Considering that some added sites may be too close to the original sites, therefore, as shown in Figure 3(b), buffer areas were created using the original sites as centres with a radius R (R was set at 3 km in this study). Local centres within the buffers were not classified as newly added sites, while those outside the buffers were selected as such.

The comprehensive vaccination site set consists of both original sites and newly added sites. Based on the mathematical expression (Eq. 13), the optimal number of vaccination sites can be determined and the optimized sites *OptS*(p') among the total vaccination sites identified. The abandoned vaccination sites (denoted as *AbaS*) among the original sites can be calculated as follows:

$$AbaS = OriS - OptS(p') \cap OriS. \quad \text{(Eq. 15)}$$

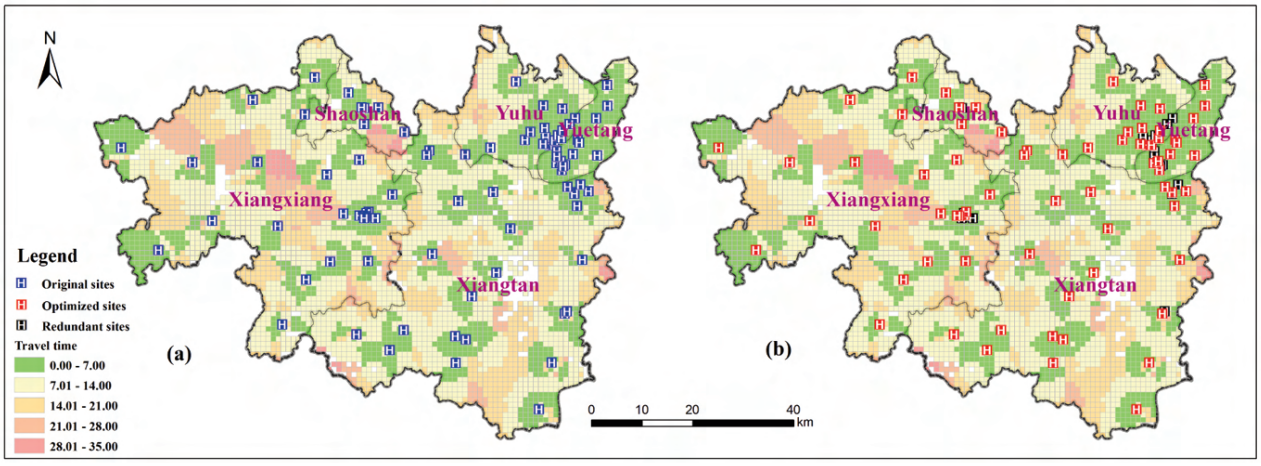

Figure 3. Illustration of temporary vaccination site extraction.

Results

Results of spatial accessibility based on hybrid travel time

Statistical results for walking time thresholds across each age group are presented in Figure 4(a-c). The mean acceptable walking time were 14.4, 29.4 and 21.3 min for children, those at middle age and the elderly, respectively, with Standard Deviations (SD) of 6.5, 14.7, and 8.7 min respectively. Compared to the children, both those at middle age and the elderly can endure longer walking time. Furthermore, the frequency histogram in Figure 3 suggests that the walking time thresholds for each age group approximate a near-Gaussian distribution. Consequently, according to Eq. 4 and Eq. 5, the probabilities for selecting different travel modes can be calculated, as depicted in Figure 4(d).

Based on the questionnaire survey recording the walking speed for each individual and the road network characteristic (such as speed limit in the study area), the mean walking and driving speed for different age groups were calculated as detailed in Table 1. The walking speed for the children was found to be 2.74 km/h, which is lower than those for the middle age people (3.89 km/h) and the elderly (3.28 km/h).

The spatial distribution of hybrid travel time exhibited a distinct clustering pattern (Figure 5(a)). High and low-value spatial clusters were detected in each county, with areas of high values primarily located around the vaccination sites. The statistical results, including the average travel time and standard deviation for each county, are shown in Figure 6. The overall average travel time across the whole study area was found to be 7.4 min. Shaoshan County exhibited the highest accessibility, with an average travel time of 10.31 min to vaccination sites, followed by Xiangxiang County at 9.5 min and Xiangtan County at 8.9 min. The Yuetang and Yuhu districts demonstrated notably shorter average travel times of 4.4 and 5.4 min, respectively, indicating easier access for residents. The SD serves as a measure of spatial accessibility inequity within each county or subarea. The Yuetang and Yuhu districts have relatively small SDs of 4.0 and 7.1 min, respectively, which are lower than the average for the study area of 12.3 min, suggesting fairer spatial accessibility within these regions. Conversely, SDs for the other three districts exceed the average for the study area, highlighting greater inequity in accessibility.

Results of spatial optimization for vaccination sites

According to the definition of scenario 1, various numbers of vaccination sites were selected, and their corresponding optimal distribution among the original vaccination sites determined. Figure 7(a) illustrates the average travel time associated with different numbers of vaccination sites, where it can be observed that the average travel time progressively increases as the number of vaccination sites decreases. Based on the mathematical expression (Eq. 13), the optimal number of reasonable vaccination sites would be 71, as all increasing rates prior to this point were greater than 0.1%, while those afterwards less than 0.1%. The corresponding distribution is shown in Figure 5(b). A total number of 21 vaccination sites were identified as redundant sites (marked as black symbols in Figure 5(b)).

As mentioned under the heading "the *p*-median problem in multiple scenario" utilizing travel time and population spatial dis-

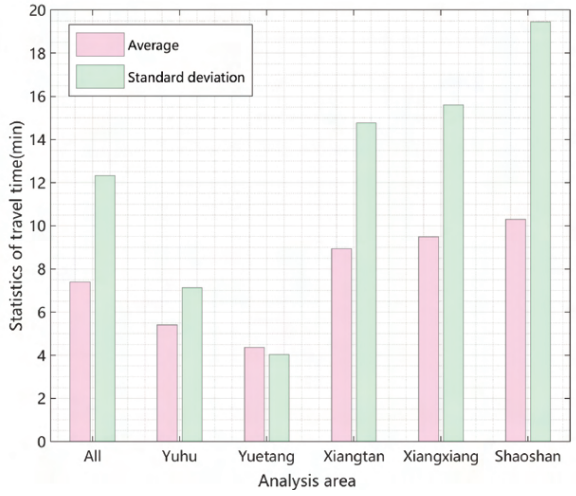

Figure 4. Statistical result giving the probability for selecting the driving mode with different walking time thresholds.

Table 1. Average speed of travel modes for different age groups.

Average speed of travel modes	Group		
	Children	Middle age	Elderly
Walking speed $u(i)$ (km/h)	2.74	3.89	3.28
Driving speed $v(i)$ (km/h)	40	40	40

tribution, four types of spatial patterns were identified: High-High, High-Low, Low-Low and Low-High areas, to determine newly added vaccination sites. To distinguish low spatial accessibility and high population density, the thresholds were set at 15 min and 500 per km^2 (Pinto & Akhavan, 2022), respectively. Newly added sites identified based on the center of Low-High areas with low accessibility (greater than 15 min) and high population density (exceeding 500 per km^2). A total of 70 newly added sites were identified. The spatial distribution of these newly added sites is shown in Figure 8(a).

Based on the overall number of sites including the original (92) and the newly added ones (70), the optimal results for different numbers of sites were calculated. As shown in Figure 7(b), the average travel time gradually decreases with an increasing number of sites. The optimal number of the optimized sites was found to be 124, which satisfies the 0.1% threshold condition. The spatial distribution of the optimized and abandoned sites is shown in Figure 8(b). To clearly understand the differences in spatial optimization across various scenarios, five key feature points were extracted from the change curve depicted in Figure 9. Point P_1(92, 7.39) corresponds to the average travel time 7.4 min achieved with the original 92 vaccination sites. Points P_2(71, 7.47) and P_5(124, 5.81) were obtained in the first and second scenarios, respectively. The average travel time (7.4 min) of point P_3 is nearly identical to that of point P_1, indicating that achieving the same average travel time with the original 92 sites requires only 53 sites after newly adding sites. Point P_4(92, 6.14), which results from optimizing the distribution after adding new sites, maintains the same number of vaccination sites as point P_1(92, 7.39). However, the average travel time at point P_4(6.1 min) is obviously lower than that at point P_1(7.4 min). This further confirms that the original distribution of vaccination sites would be unreasonable and that spatial optimization could reduce the overall comprehensive travel time for residents to access vaccination sites.

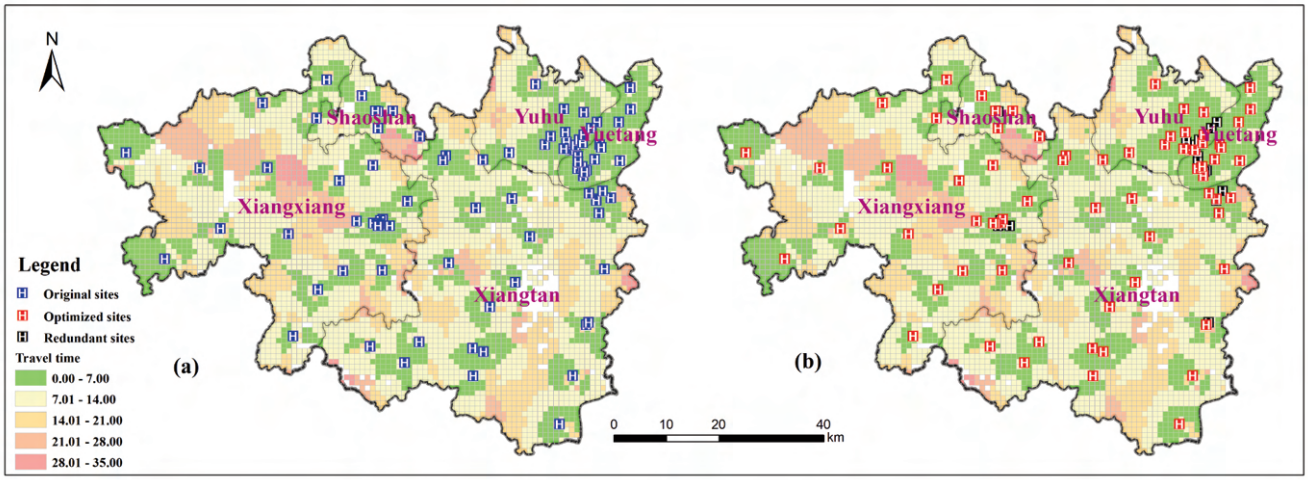

Figure 5. Spatial distribution of accessibility and optimization result. (**a**) Spatial distribution of accessibility for existing sites; (**b**) optimization result of original sites in scenario 1.ds.

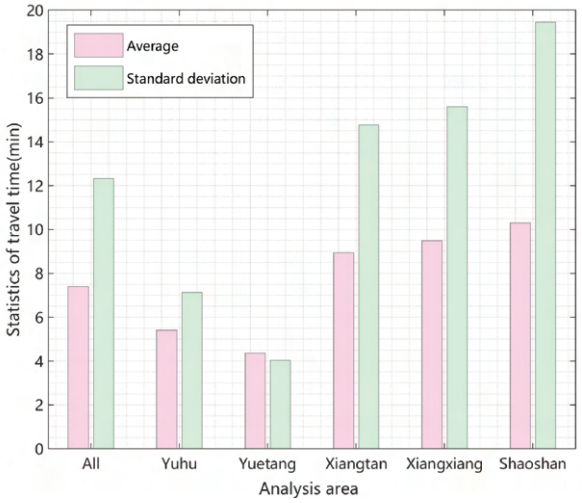

Figure 6. Statistics of travel time for different areas.

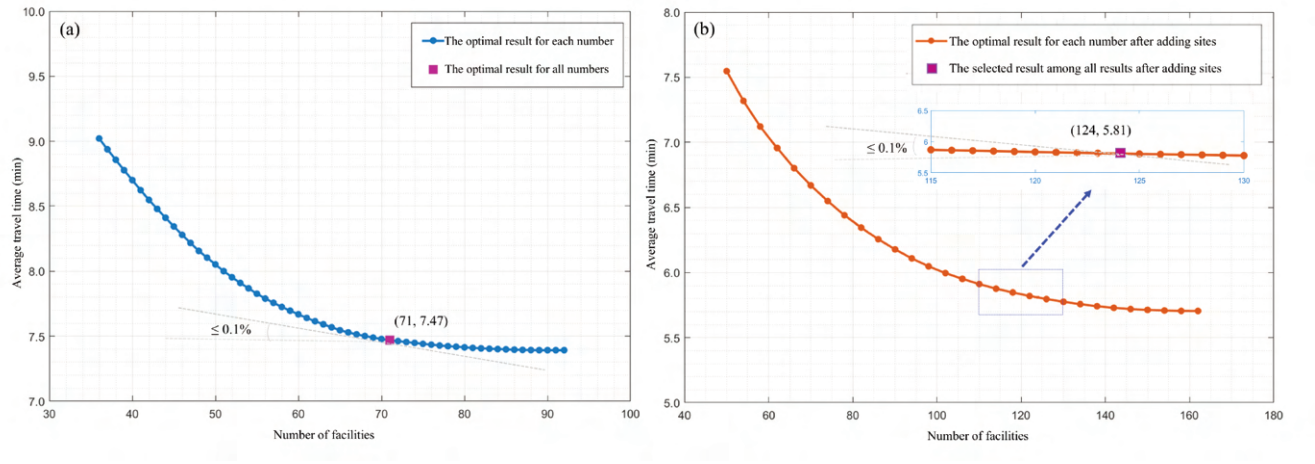

Figure 7. Change curve of optimal average travel time for each number. (**a**) Without newly added sites; (**b**) with newly added sites.

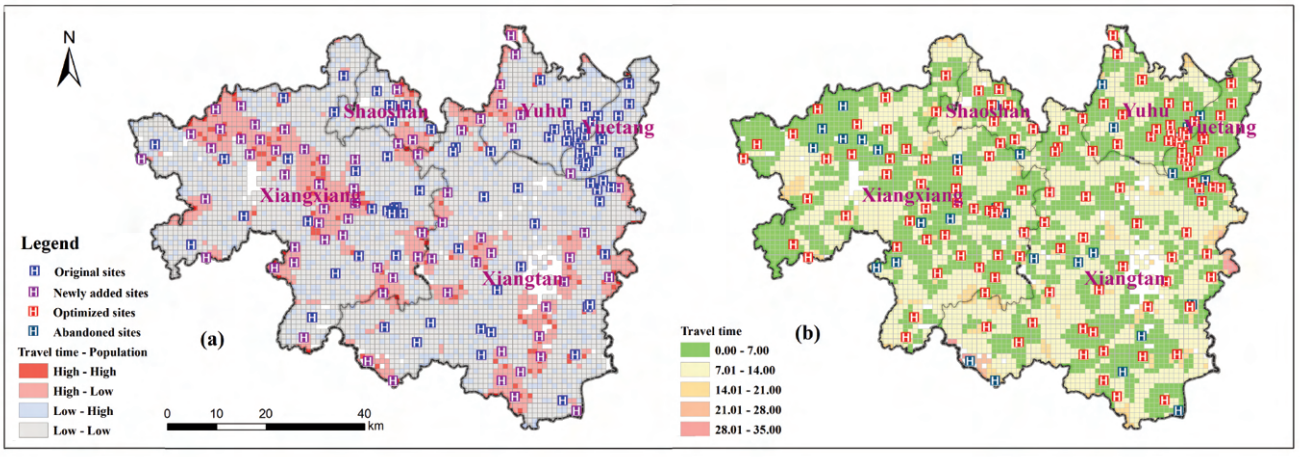

Figure 8. Spatial distribution and optimization results. (**a**) Spatial distribution of original sites and newly added sites; (**b**) optimization results for original sites and newly added sites in scenario 2.

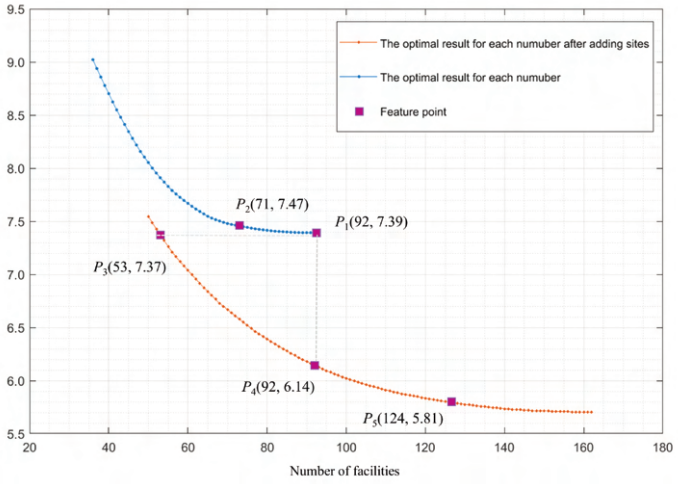

Figure 9. Comprehensive results in multiple scenarios.

Discussion

Spatial accessibility serves as a key metric for evaluating the equity of vaccination site distribution and is fundamental to optimizing site locations, which is a critical strategy for controlling infectious diseases, encompassing essential elements such as spatial supply, demand and their interdependencies. This study primarily focused on optimizing the spatial locations of vaccination sites from the viewpoint of spatial accessibility. In contrast to existing research on the spatial optimization of vaccination sites, our contribution was twofold: first, we employed a hybrid travel time metric to assess spatial accessibility; second, we investigated optimization solutions across various scenarios.

On the basis of hybrid travel time, spatial accessibility to vaccination sites was obtained and spatial inequality identified. The statistical results show that the average travel time in the Yuetang and Yuhu districts is lower than that of the entire study. Additionally, the SD of the average comprehensive travel time in these districts is also lower than in other areas, indicating that spatial accessibility within these districts is relatively equitable. Actually, the Yuetang and Yuhu districts, the primary population centers in Xiangtan, benefit from a high concentration of vaccination sites and a well-developed transportation infrastructure that contributes to their accessibility. Conversely, areas with lower urbanization rates and lower population densities, coupled with inadequate transportation facilities, hinder public access to vaccination sites.

This study obtained optimization solutions for the spatial distribution of vaccination sites across various scenarios. In scenario 1, redundant sites are considered as elements of the original vaccination sites, whose existence would not significantly impact average accessibility. The increasing threshold is used to identify whether or not a site is redundant. By setting the increasing threshold at 0.1%, a total number of 21 redundant sites were identified in the study area and they were mainly located in the urban areas. Should the number of original vaccination sites be reduced, these 21 sites should be prioritized based on spatial accessibility. Similarly, in scenario 2, in which the spatial optimization with the consideration of newly added sites was examined, the increasing threshold was used to determine the final results, a total of 124 sites were identified among the original and newly added sites. It is important to note that scenario 1 aimed to divide original vaccination sites into redundant and optimized/reasonable vaccination sites, whose input is the spatial distribution of these two types of vaccination sites, while scenario 2 tended to input the spatial distribution of optimized vaccination sites consisting of some original and some newly added ones.

There are still a series of limitations that should be pointed out. Firstly, in this study, only two travel modes were considered when defining hybrid travel time and the selection of travel modes was assumed to be solely related to age. Actually, travel modes are more diverse and complex, with public or shared transportation being common options. Further, the selection of travel modes is influenced by multiple factors indicating that a more comprehensive integration of human mobility patterns into spatial accessibility measurement is necessary. This research employed the cumulative distribution function of the Gaussian distribution to characterize the probability of travel mode selection. However, more suitable methods for measuring choice probability require further exploration. Secondly, the objective of spatial optimization was to minimize total travel time. However, the medical or economic cost associated with adding new vaccination sites is also a critical element for newly adding vaccination sites. Future research should explore multi-objective optimization that incorporates time, medical and economic factors. Additionally, in scenario 1, the definition of redundant vaccination sites is qualitative and to measure no significant impact on total cost is uncertain based on the increment threshold, which can be found from the mathematical expression (Eq. 13). Obviously, the results may vary with different thresholds. In this study, to simplified calculations by using just one threshold (0.1%), something which necessitates further discussion on how to select thresholds.

Conclusions

This study investigated the spatial optimization for vaccination sites based on heterogeneous travel modes across two distinct scenarios (one without additional sites and another with newly added) by applying population-weighted hybrid travel time. Compared to other distance indicators, hybrid travel time can effectively capture the mixed distance situation with the consideration of different travel modes and their selected probabilities. Importantly, this study is not only applicable to spatial optimization of vaccination sites, but can also be used for to find the best spatial distribution of a wide variety of other geographical, infrastructural elements. In the case study of Xiangtan, China, the spatial optimization solution offers valuable insights for the government in preventing and controlling infectious diseases.

References

Amritpal KK, Victoria F, Rizwan S, 2019. Spatial accessibility to primary healthcare services by multimodal means of travel: synthesis and case study in the city of Calgary. Int J Env Res Pub Health 16:170.

Chen X, Jia P, 2019. A comparative analysis of accessibility measures by the two-step floating catchment area (2SFCA) method. Int J Geogr Inf Sci 33:1739–58.

Chen Y, Tao R, Downs J, 2022. Location optimization of COVID-19 vaccination sites: Case in Hillsborough County, Florida. Int J Env Res Pub He 19:12443.

Church RL, Murray A, 2009. Business site selection, location modeling and GIS. Hoboken, NJ: John Wiley & Sons.

Daskin MS, 1995. Network and discrete location: Models, algorithms, and applications. New York, NY: John Wiley & Sons.

Fei W, Linghong Y, Weigang Z, Ruihan Z, 2024. Dynamic location model for designated COVID-19 hospitals in China. Geospatial Health 19:1310.

Grauer J, Löwen H, Liebchen B, 2020. Strategic spatiotemporal vaccine distribution increases the survival rate in an infectious disease like COVID-19. Sci Rep-UK 10:21594.

Guhlincozzi AR, Lotfata A, 2022. Travel distance to flu and COVID-19 vaccination sites for people with disabilities and age 65 and older, Chicago metropolitan area. J Health Res 36:859–66.

Hakimi SL, 1964. Optimum location of switching centers and the absolute centers and medians of a graph. Oper Res 12:450–59.

Huang L, Yang Y, Chen H, Zhang Y, Wang Z, He L. 2022. Context-aware road travel time estimation by coupled tensor decompo-

sition based on trajectory data. Knowl-Based Syst 245:108596.
Huang J, Chen Y, Liu G, Tu W, Bergquist RP, Ward M, Zhang J, Xiao S, Hong J, Zhao Z, Li X, Zhang Z, 2023. Optimizing allocation of colorectal cancer screening hospitals in Shanghai: a geospatial analysis. Geospatial Health, 18:1152.
Lee BY, Brown ST, Korch GW, Cooley PC, Zimmerman RK, Wheaton WD, Zimmer SM, Grefenstette JJ, Bailey RR, Assi TM, 2010. A computer simulation of vaccine prioritization, allocation, and rationing during the 2009 H1N1 influenza pandemic. Vaccine 28:4875–79.
Lee J, Miller HJ, 2018. Measuring the impacts of new public transit services on space-time accessibility: An analysis of transit system redesign and new bus rapid transit in Columbus, Ohio, USA. Appl Geogr 93:47–63.
Liang Y, Xie Z, Chen S, Xu Y, Xin Z, Yang S, 2023. Spatial accessibility of urban emergency shelters based on GA2SFCA and its improved method: a case study of Kunming, China. J Urban Plan Dev 149:05023013.
Liu CL, Yu RL, 2012. Spatial accessibility of road network in Wuhan metropolitan area based on spatial syntax. J Geogr Inf Syst 4:128–35.
Liu D, Kwan MP, Kan Z, Song Y, Li X, 2022. Racial/ethnic inequity in transit-based spatial accessibility to COVID-19 vaccination sites. J Racial Ethn Health 10:1533–41.
Luo W, Qi Y, 2009. An enhanced two-step floating catchment area (E2SFCA) method for measuring spatial accessibility to primary care physicians. Health Place 15:1100–07.
McGrail MR, 2012. Spatial accessibility of primary health care utilizing the two-step floating catchment area method: An assessment of recent improvements. Int J Health Geogr 11:50.
Medlock J, Galvani AP, 2009. Optimizing influenza vaccine distribution. Science 325:1705–08.
Park J, Goldberg DW, 2021. A Review of recent spatial accessibility studies that benefitted from advanced geospatial information: Multimodal transportation and spatiotemporal disaggregation. ISPRS Int J Geo-Inf 10:532.
Pinto F, Akhavan M, 2022. Scenarios for a post-pandemic city: Urban planning strategies and challenges of making "Milan 15-minutes city." Transp Res Procedia 60:370–77.
Polo G, Acosta CM, Dias RA, 2013. Spatial accessibility to vaccination sites in a campaign against rabies in so Paulo city, Brazil. Prev Vet Med 111:10–6.
Qi F, Barragan D, Rodriguez MG, Lu J, 2022. Evaluating spatial accessibility to COVID-19 vaccine resources in diversely populated counties in the United States. Front Public Health 10:895538.
Sah P, Medlock J, Fitzpatrick MC, Singer BH, Galvani AP, 2018. Optimizing the impact of low-efficacy influenza vaccines. P Natl Acad Sci USA 115:5151–56.
Scroggins S, Goodson J, Afroze T, Shacham E, 2023. Spatial Optimization to improve COVID-19 vaccine allocation. Vaccines 11:64.
Snyder S, Haight RG, 2016. Application of the maximal covering location problem to habitat reserve site selection: A review. Int Regional Sci Rev 39:28–47.
Soukhov A, Páez A, Higgins CD, Mohamed M, 2023. Introducing spatial availability, a singly-constrained measure of competitive accessibility. PLoS One 18:e0278468.
Tao R, Downs J, Beckie TM, Chen Y, McNelley W, 2020. Examining spatial accessibility to COVID-19 testing sites in Florida. Ann Gis 26:319–27.
Tao Y, Shea K, Ferrari M, 2018. Logistical constraints lead to an intermediate optimum in outbreak response vaccination. Plos Comput Biol 14:e1006161.
Wallinga J, van Boven M, Lipsitch M, 2010. Optimizing infectious disease interventions during an emerging epidemic. P Natl A Sci 107:923–28.
Wang S, Wang M, Liu Y, 2021. Access to urban parks: comparing spatial accessibility measures using three GIS-based approaches. Comput Environ Urban Syst 90:101713.
Wei J, Zhang W, Doherty M, Wallace ZS, Sparks JA, Lu N, Li XX, Zeng C, Lei GH, Zhang YQ, 2023. Comparative effectiveness of BNT162B2 and chAdOx1 nCov-19 vaccines against COVID-19. BMC Med 21:78.
Xiao N, Murray AT, 2019. Spatial optimization for land acquisition problems: a review of models, solution methods, and GIS support. T Gis 23:645–71.
Xiao T, Ding T, Zhang X, Tao Z, Liu Y, 2022. Spatial accessibility to sports facilities in Dongguan, China: A multi-preference gaussian two-step floating catchment area method. Appl Spat Anal Polic 15:1093–14.
Yang W, Deng M, Li C, Huang J, 2020. Spatio-temporal patterns of the 2019-ncov epidemic at the county level in Hubei province, China. Int J Env Res Pub He 17:2563–73.
Yang W, Wang F, You Y, Wan X, Cheng S, Fang Z, 2024. Evaluating spatial accessibility to COVID-19 vaccination sites based on fine-scale population distributions and heterogeneous travel modes: A case study in Xiangtan, China. Appl Spat Anal Polic 17:867–90.
Yu B, Wang H, Shan W, Yao B, 2018. Prediction of bus travel time using random forests based on near neighbors. Comput-aided Civ Inf 33:333–50.
Zhou S, Zhou S, Zheng Z, Lu J, 2021. Optimizing spatial allocation of COVID-19 vaccine by agent-based spatiotemporal simulations. GeoHealth 5:e2021GH000427.